Available online at www.sciencedirect.com
ScienceDirect
Journal of Solid State Chemistry 181 (2008) 1176–1183
JOURNAL OF SOLID STATE CHEMISTRY
www.elsevier.com/locate/jssc

Spatially selected synthesis of LaF_3 and Er^{3+}-doped CaF_2 crystals in oxyfluoride glasses by laser-induced crystallization

M. Kusatsugu, M. Kanno, T. Honma, T. Komatsu*

Department of Materials Science and Technology, Nagaoka University of Technology, 1603-1 Kamitomioka-cho, Nagaoka 940-2188, Japan

Received 8 December 2007; received in revised form 22 February 2008; accepted 26 February 2008
Available online 29 February 2008

Abstract

Oxyfluoride glasses with a small amount of NiO are prepared using a conventional melt quenching technique, and the spatially selected crystallization of LaF_3 and CaF_2 crystals is induced on the glass surface by irradiations of continuous wave lasers with a wavelength of $\lambda = 1064$ or 1080 nm. Dots and lines including LaF_3 crystals are patterned by heat-assisted (300 °C) laser irradiations ($\lambda = 1064$ nm) with a power of $P = 1$ W and an irradiation time of 10 s for dots and a scanning speed of $S = 5\,\mu$m/s for lines. Lines consisting of CaF_2 crystals are also patterned in an ErF_3-doped oxyfluoride glass by laser irradiations ($\lambda = 1080$ nm) with a power of $P = 1.7$ W and a scanning speed of $S = 2\,\mu$m/s, and the incorporation of Er^{3+} ions into CaF_2 crystals is confirmed from micro-photoluminescence spectrum measurements. It is proposed that the lines patterned by laser irradiations in this study are consisted of the composite of LaF_3 or CaF_2 nanocrystals and SiO_2-based oxide glassy phase. It is demonstrated that a combination of Ni^{2+}-dopings and laser irradiations is effective in spatially selected local crystallizations of fluorides in oxyfluoride glasses.

Keywords: Oxyfluoride glass; Laser-induced crystallization; LaF_3 nanocrystals; CaF_2 nanocrystals

1. Introduction

Fluoride glasses and crystals are desirable hosts for optically active ions because of their transparencies in the range from the near ultra-violet (UV) to the middle of infrared (IR), low phonon energy, and large rare-earth ion (RE^{3+}) solubility. Generally, fluoride materials have, however, drawbacks to chemical and thermal stabilities, limiting in the use of optical devices. For this problem, Wang and Ohwaki [1] gave a solution. That is, they proposed oxyfluoride-based crystallized glasses (glass-ceramics) consisting of fluoride nanocrystals. RE^{3+} ions are incorporated into fluoride nanocrystals being embedded in SiO_2-based oxide glass matrices, and thus oxyfluoride-based crystallized glasses can maintain good chemical and thermal stabilities. After their first proposal, numerous researches on the fabrication and optical properties of transparent RE^{3+}-doped oxyfluoride-based crystallized glasses have been reported so far [2–9].

Usually, crystallized glasses are fabricated using well-controlled heat treatments in an electric furnace and desired crystals are formed on the surface or in the interior of glass. In this kind of heat treatment methods, it is generally difficult to induce crystallization in spatially selected regions. It is of interest and of important to develop crystallized glasses, in which functional crystals are induced in a desired part in a given glass matrix. Laser irradiation of glass has been regarded as a process for spatially selected structural modification and crystallization in glass, and recently, various studies in laser-induced structural changes have been carried out. The present authors' group has developed techniques of laser-induced crystallization in glass, i.e., rare-earth or transition metal atom heat processing method, and has succeeded in patterning crystal lines consisting of nonlinear or ferroelectric crystals such as β-BaB_2O_4, $Ba_2TiGe_2O_8$, and $LiNbO_3$ [10–16].

It is of particular interest to irradiate laser to oxyfluoride glasses and to develop crystallized glasses consisting of

*Corresponding author. Fax: +81 258 47 9300.
E-mail address: komatsu@mst.nagaokaut.ac.jp (T. Komatsu).

0022-4596/$ - see front matter © 2008 Elsevier Inc. All rights reserved.
doi:10.1016/j.jssc.2008.02.026

fluoride crystals in a desired part, e.g., patterning of fluoride crystal dots and lines in oxyfluoride glass matrices. Such a patterning would induce other potentials for optical device applications of oxyfluoride glasses with fluoride nanocrystals. There has been, however, no report on the spatially selected formation of fluoride crystals using direct laser-induced crystallization techniques in oxyfluoride glasses. In this study, we focus our attention on the spatially selected synthesis of LaF_3 and CaF_2 nanocrystals in oxyfluoride glasses by using a laser-induced crystallization technique. We apply transition metal atom (Ni^{2+} ion) heat processing to NiO-doped oxyfluoride glasses and demonstrate that it is possible to form LaF_3 and Er^{3+}-doped CaF_2 nanocrystals in a desired part on the glass surface. Recently, Mekhlouf et al. [17] have reported the local crystallization of LaF_3 nanocrystals in an oxyfluoride glass using a combination technique of ultraviolet laser (wavelength: 244 nm) irradiations and heat treatments at temperatures below the glass transition temperature.

2. Experimental

Various papers on the fabrication and optical properties of transparent oxyfluoride-based crystallized glasses consisting of LaF_3 or CaF_2 nanocrystals have been reported so far [2–8]. Considering the previous papers [2–8], we used the following glasses, i.e., $40SiO_2$–$25Al_2O_3$–$20Na_2O$–$15LaF_3$–xNiO (mol%), $x=0$ and 3, glasses for the synthesis of LaF_3 nanocrystals, $43SiO_2$–$22Al_2O_3$–5CaO–13NaF–$17CaF_2$–xNiO, $x=0$ and 3, glasses for CaF_2 nanocrystals, and $43SiO_2$–$22Al_2O_3$–5CaO–13NaF–$17CaF_2$–3NiO–0.5ErF3 glass for Er^{3+}-doped CaF_2 nanocrystals, in which NiO was added as an absorption heating source of lasers.

The glasses were prepared using a conventional melt quenching method. Commercial powders of raw materials such as SiO_2, Al_2O_3, Na_2CO_3, LaF_3, CaF_2, ErF_3, and NiO were mixed and melted in a platinum crucible with a lid at 1400 °C for 1 h or 1.5 h in air in an electric furnace. The melts were poured onto an iron plate and pressed to a thickness of ~1.5 mm with another iron plate. The glass transition, T_g, and crystallization peak, T_p, temperatures were determined using differential thermal analyses (DTA) at a heating rate of 10 or 20 K/min. Optical absorption spectra were measured in the wavelength range of 250–2000 nm using a spectrometer (SHIMADZU U-3120). The glasses were heat-treated at various temperatures for 1 or 2 h in an electric furnace, and crystalline phases present in the heat-treated samples were examined by X-ray diffraction (XRD) analyses (Cu $K\alpha$ radiation) at room temperature.

The glasses were mechanically polished to a mirror finish with CeO_2 powders. Cw Nd:YAG lasers with $\lambda=1064$ nm or Yb:YVO_4 fiber lasers with $\lambda=1080$ nm were irradiated onto the surface of the glass using an objective lens (20 magnification). The sample was put on the stage and mechanically moved during laser irradiations to construct crystal dots and lines. Crystal dots and lines were observed with a confocal scanning laser microscope (OLYMPUS-OLS 3000) and examined by micro-Raman scattering spectrum measurements (Tokyo Instruments Co., Nanofinder; Ar^+ laser 488 nm) and XRD analyses. For the lines patterned in Er^{3+}-doped glasses, photoluminescence spectra of Er^{3+} ions were measured.

3. Results and discussion

3.1. Formation and some properties of glasses

The XRD measurements for the melt-quenched samples were carried out, and only halo patterns without any sharp peaks were observed. In DTA patterns, all samples showed endothermic peaks due to the glass transition. It is, therefore, confirmed that all samples prepared in this study are glass. The values of T_g and T_p estimated from the DTA curves are summarized in Table 1. It is found that all glasses show similar values of $\sim T_g = 570$ °C irrespective of LaF_3 and CaF_2 components. These results suggest that the glass transition temperature of oxyfluoride glasses based on SiO_2–Al_2O_3–Na_2O or CaO would be mainly determined by the total amount of SiO_2 and Al_2O_3. On the other hand, it is found that crystallization behaviors depend largely on the other components besides of SiO_2 and Al_2O_3.

The optical absorption spectra at room temperature for the glasses of $40SiO_2$–$25Al_2O_3$–$20Na_2O$–$15LaF_3$–xNiO (mol%), $x=0$ and 3, are shown in Fig. 1 as examples. The glasses without NiO and with 3NiO addition are designated here as Glass A(LaF_3) and Glass B(LaF_3), respectively. In Glass B(LaF_3) with 3NiO addition, the absorption band with a strong intensity at around 430 nm and a broad band centered at round 850 nm are observed. These peaks are typical for Ni^{2+} ions in glass [18–21]. It is well known that the coordination of Ni^{2+} ions is very sensitive to their ligand field environments, i.e., ionic-bonded octahedral coordinations in acidic (low optical basicity) glasses and covalent-bonded tetrahedral coordinations in high basicity glasses [19], consequently giving the change in the ratio of the amount of octahedral and tetrahedral coordinated Ni^{2+} ions in glass [20]. The spectrum shown in Fig. 1, however, suggests that Ni^{2+} ions in the glasses prepared in this study have mainly octahedral coordination environments, because the peaks at around 430 and 850 nm are typical for octahedral coordinated Ni^{2+} ions in glass [21]. The optical absorption coefficient at $\lambda=1064$ nm for Glass B(LaF_3) with 3NiO is $\alpha=4.0\,cm^{-1}$. Similar optical absorption spectra were observed for the glasses of $43SiO_2$–$22Al_2O_3$–5CaO–13NaF–$17CaF_2$–xNiO, $x=0$ and 3. These glasses without NiO and with 3NiO addition are designated here as Glass C(CaF_2) and Glass D(CaF_2), respectively. The value of $\alpha=5.1\,cm^{-1}$ at $\lambda=1080$ nm was obtained for Glass D(CaF_2) with 3NiO addition.

Table 1
Chemical compositions, glass transition, T_g, and crystallization peak, T_p, temperatures of the glasses prepared in the present study

Sample	Glass composition (mol)	T_g (°C)	T_p (°C)
Sample A(LaF_3)	$40SiO_2$–$25Al_2O_3$–$20Na_2O$–$15LaF_3$	567	–
Sample B(LaF_3)	$40SiO_2$–$25Al_2O_3$–$20Na_2O$–$15LaF_3$–3NiO	576	819
Sample C(CaF_2)	$43SiO_2$–$22Al_2O_3$–5CaO–13NaF–$17CaF_2$	570	630
Sample D(CaF_2)	$43SiO_2$–$22Al_2O_3$–5CaO–13NaF–$17CaF_2$–3NiO	573	617
Sample E(CaF_2)	$43SiO_2$–$22Al_2O_3$–5CaO–13NaF–$17CaF_2$–3NiO–$0.5ErF_3$	575	635

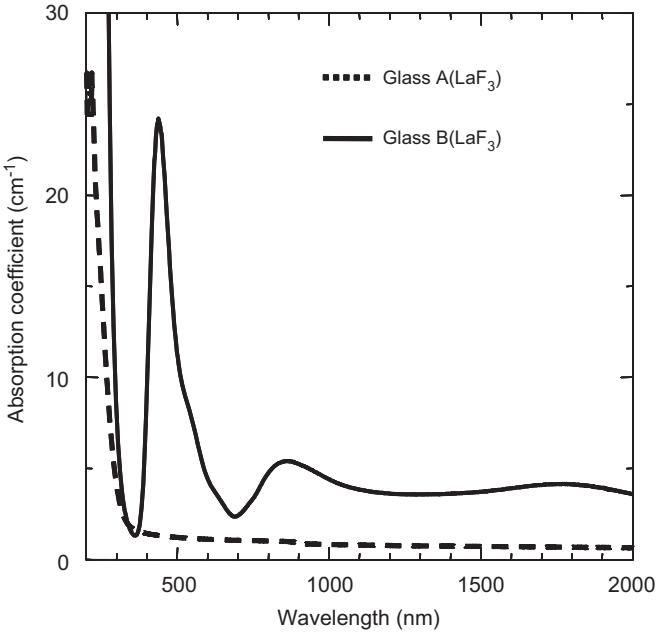

Fig. 1. Optical absorption spectra at room temperature for Glass A(LaF_3) and Glass B(LaF_3).

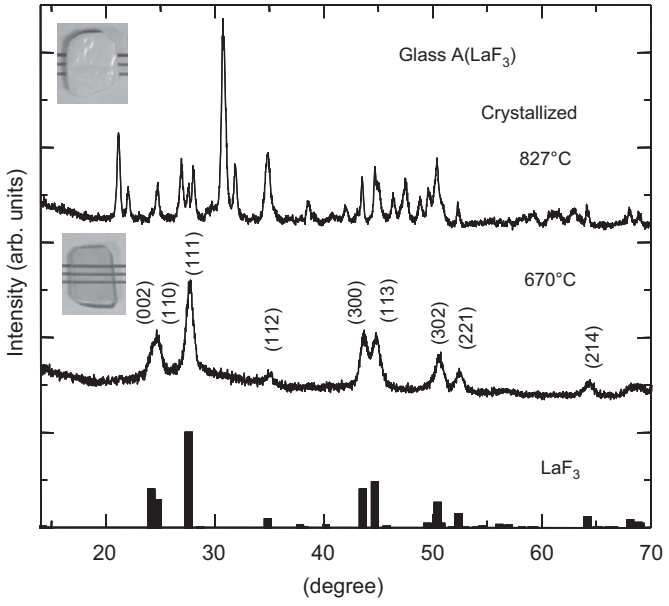

Fig. 2. Powder XRD patterns at room temperature for the crystallized samples of Glass A(LaF_3). The insets are optical photographs for the samples.

3.2. *Crystallization of LaF_3 and CaF_2 nanocrystals in an electric furnace*

Prior to the spatially selected crystallization of LaF_3 or CaF_2 crystals on the glass surface by laser irradiations, usual crystallization behaviors in an electric furnace were examined. It is important to clarify the formation temperature of LaF_3 or CaF_2 fluoride nanocrystals and the crystallization temperature of the oxide glass part.

The powder XRD patterns for the crystallized samples in Glass A(LaF_3) without NiO addition are shown in Fig. 2. It is seen that LaF_3 crystals are formed in the sample heat-treated at 670 °C. The average particle size of LaF_3 crystals was estimated to be around 68 nm from the peak width of XRD pattern by using the Sherrer's equation, keeping a good transparency in the crystallized sample. In the sample heat-treated at 827 °C, other crystalline phases (not identified at this moment) are formed beside LaF_3 crystals, and the sample became opaque. It is considered that the oxide glass part of SiO_2–Al_2O_3–Na_2O crystallizes in this heat treatment. Here, we propose to call this crystallization "crystallization of host oxide glass".

The powder XRD patterns for the crystallized samples in Glass B(LaF_3) with 3NiO addition are shown in Fig. 3. LaF_3 crystals are formed in the samples obtained by heat treatments at 620–658 °C, and the average particle size of LaF_3 crystals in these samples was estimated to be 16–24 nm from the peak width of XRD patterns. As shown in Fig. 3, an unidentified crystalline phase (marked in the closed circle) is formed together with LaF_3 crystals. Interestingly, this crystalline phase disappears almost in the sample heat-treated at 700 °C, suggesting that it might be a metastable crystalline phase.

The powder XRD patterns for the crystallized samples in Glass D(CaF_2) with 3NiO addition are shown in Fig. 4. CaF_2 crystals are formed in the samples obtained by heat treatments at ~610 °C, and the average particle size of CaF_2 crystals in these samples was estimated to be 19–24 nm from the peak width of XRD patterns. It should be pointed out that any other crystalline phases except CaF_2 were not detected in these heat treatment temperatures.

The results shown in Figs. 3 and 4 clearly demonstrate that LaF_3 or CaF_2 nanocrystals are formed as the initial

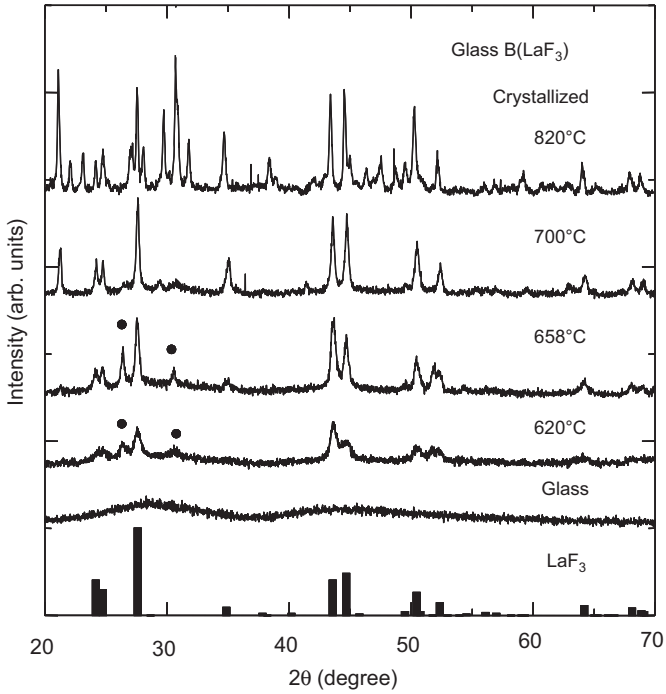

Fig. 3. Powder XRD patterns at room temperature for the crystallized samples of Glass B(LaF_3). The closed circle (•) corresponds to an unidentified phase.

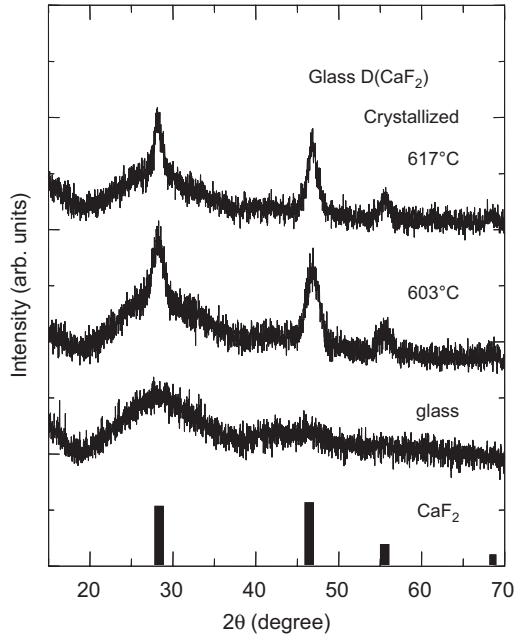

Fig. 4. Powder XRD patterns at room temperature for the crystallized samples of Glass D(CaF_2).

crystalline phase even in oxyfluoride glasses with a small addition of 3NiO, as similar to oxyfluoride glasses with no NiO additions reported so far [2–8]. In transparent oxyfluoride crystallized glasses, the effect of transition metal oxides such as NiO on the nanocrystallization has not been reported so far. It is important to clarify whether Ni^{2+} ions are incorporated into LaF_3 or CaF_2 nanocrystals or not. The ionic radii of La^{3+}, Ca^{2+}, and Ni^{2+} (octahedral) are 0.103, 0.100, and 0.069 nm, respectively [22]. That is, there is a large difference in their ionic radii, suggesting that an incorporation of Ni^{2+} ions into LaF_3 or CaF_2 nanocrystals would be very small, even if occurred. This point will be discussed again in the later section.

3.3. Crystallization of LaF_3 crystals by laser irradiation

As stated in the above section, it was clarified that LaF_3 nanocrystals are formed as the initial crystalline phase in the crystallization of 3NiO-doped oxyfluoride glass. We tried to pattern dots and lines consisting of LaF_3 crystals on the glass surface by irradiations of cw Nd:YAG laser with $\lambda = 1064$ nm. In the laser irradiation experiments, a heat-assisted method was applied, in which glass samples were put on the sample stage heated at 300 °C during laser irradiations. This temperature of 300 °C is far below from the glass transition temperature of $T_g = 576$ °C. Without a heat-assisted method, it was impossible to induce the crystallization of LaF_3 in our oxyfluoride glass by our laser irradiations. A heat-assisted method has also an effect in the depression of sudden sample break due to thermal shock during laser irradiations.

The confocal scanning laser micrographs for Glass B(LaF_3) obtained by Nd:YAG laser irradiations with a power of $P = 1$ W and irradiation times of $t = 10$ and 60 s are shown in Fig. 5. The bumps are observed in both samples, indicating that a structural change is induced by

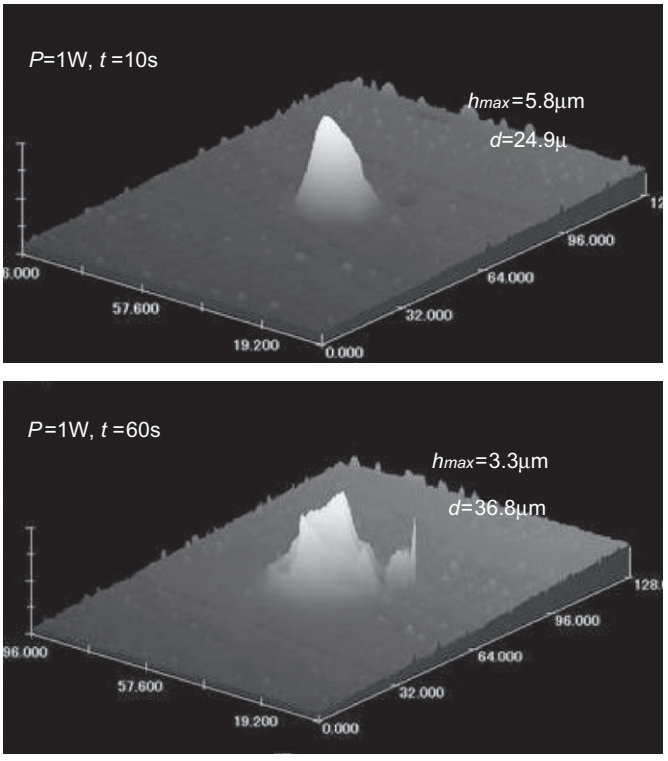

Fig. 5. Scanning confocal laser micrographs for the samples obtained by Nd:YAG laser irradiations with a laser power of $P = 1$ W and for 10 and 60 s in Glass B(LaF_3).

laser irradiations. The height, h_{max}, and diameter, d, of the dots are $h_{max} = 5.8\,\mu m$ and $d = 24.9\,\mu m$ for the dot obtained by laser irradiations of $t = 10\,s$ and $h_{max} = 3.3\,\mu m$ and $d = 36.8\,\mu m$ for the dot obtained by laser irradiations of $t = 60\,s$. It is found that the height of dots decreases with increasing laser irradiation time, and contrary, the diameter increases with increasing laser irradiation time. The confocal scanning laser micrograph for Glass B(LaF_3) obtained by laser irradiations with $P = 1\,W$ and a scanning speed of $S = 5\,\mu m/s$ is shown in Fig. 6. The structure change with a width of 26.8 μm and a height of 3.8 μm is observed, and it should be emphasized that the surface morphology is smooth.

The micro-Raman scattering spectra at room temperature for the dot (Fig. 5; $P = 1\,W$ and $t = 10\,s$) and line (Fig. 6; $P = 1\,W$ and $S = 5\,\mu m/s$) are shown in Fig. 7. The Raman scattering spectra for LaF_3 powders commercially available, Glass B(LaF_3) itself without any laser irradiations, and the crystallized glass (obtained by a heat treatment at 660 °C for 1 h in an electric furnace) with LaF_3 nanocrystals are also shown in Fig. 7. It is seen that LaF_3 crystals give a sharp peak at $380\,cm^{-1}$ and such a sharp peak does not exist in the glass sample. The Raman scattering spectra for the dot and line show a peak at $380\,cm^{-1}$ and are almost the same as to that for the crystallized glass. It is, therefore, concluded that the dot and line obtained by Nd:YAG laser irradiations include LaF_3 crystals. Glass B(LaF_3), i.e, $40SiO_2$–$25Al_2O_3$–$20Na_2O$–$15LaF_3$–$3NiO$, has the values of $T_g = 576$ and $T_p = 819$ °C. As shown in Figs. 1 and 5, it is obvious that LaF_3 nanocrystals are formed initially by heat treatments at temperatures above around 600 °C and then the host oxide glass part starts to crystallize at temperatures above around 700 °C. As only LaF_3 crystals are detected in the laser irradiated region, it would be concluded that the temperature of the laser irradiated region would be around 600–670 °C, i.e., at least less than 700 °C. Furthermore, the Raman scattering spectra shown in Fig. 7 for the dot and line indicate the broad peaks being typical of the glassy phase, and therefore, the dots and lines would be composites consisting of the host oxide glass phase and LaF_3 crystals.

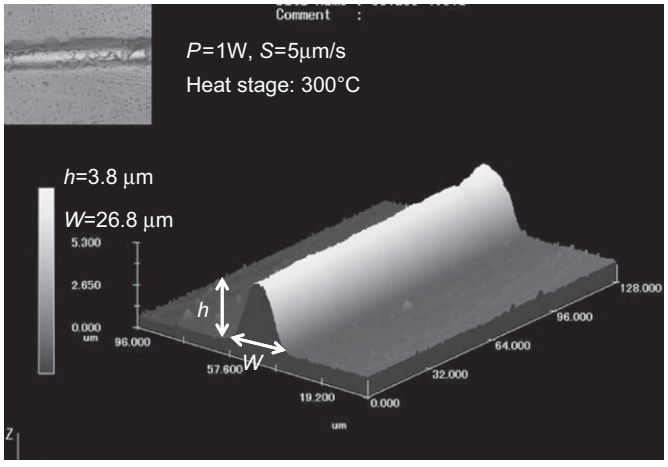

Fig. 6. Scanning confocal laser micrograph for the sample obtained by Nd:YAG laser irradiations with a laser power of $P = 1\,W$ and a scanning speed of $S = 5\,\mu m/s$ in Glass B(LaF_3).

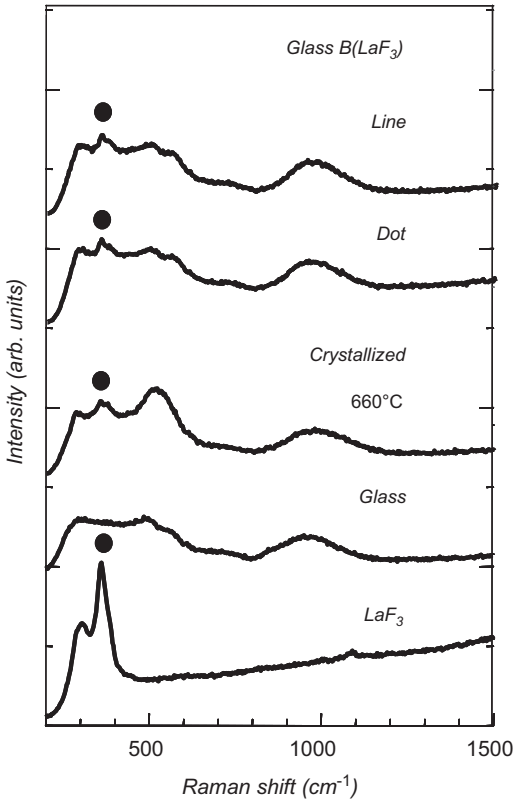

Fig. 7. Micro-Raman scattering spectra at room temperature for the dot (Fig. 5; $P = 1\,W$ and $t = 10\,s$) and line (Fig. 6; $P = 1\,W$ and $S = 5\,\mu m/s$) in Glass B(LaF_3). The data for LaF_3 powders commercially available, sample without any laser irradiations, and the crystallized glass (heat treatment at 660 °C for 1 h in an electric furnace) with LaF_3 nanocrystals are also shown.

3.4. Crystallization of Er^{3+}-doped CaF_2 crystals by laser irradiation

The laser-induced crystallization of CaF_2 crystals was also tried on the glass surface of Glass D(CaF_2) by using a Yb:YVO_4 fiber laser with $\lambda = 1080\,nm$. The polarized optical photograph and confocal scanning micrograph for the sample obtained by laser irradiations with a condition of $P = 1.7\,W$ and $S = 2\,\mu m/s$ are shown in Fig. 8. It is seen that the lines with smooth surfaces are patterned on the glass surface. The height and width of the lines are ~1 and ~3 μm, respectively. The XRD pattern for the assemblage (50 lines) of these lines is shown in Fig. 9, indicating the formation of CaF_2 crystals. From the half width of the peak at the angle of $2\theta = 47^\circ$ corresponding to the (220) plane, the particle size was estimated to be ~15 nm. That is, CaF_2 nanocrystals are induced in the NiO-doped oxyfluoride glass by laser irradiations.

The formation of CaF_2 nanocrystals was confirmed from XRD measurements in the transparent crystallized

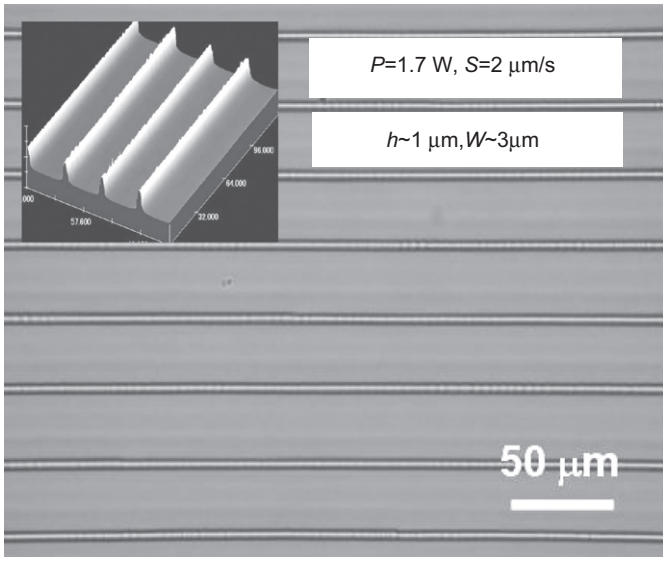

Fig. 8. Polarized optical micrograph for the lines obtained by Yb:YVO_4 laser irradiations with a laser power of $P = 1.7$ W and a scanning speed of $S = 2\,\mu m/s$ in Glass D(CaF_2). The inset is a scanning confocal laser micrograph for the sample.

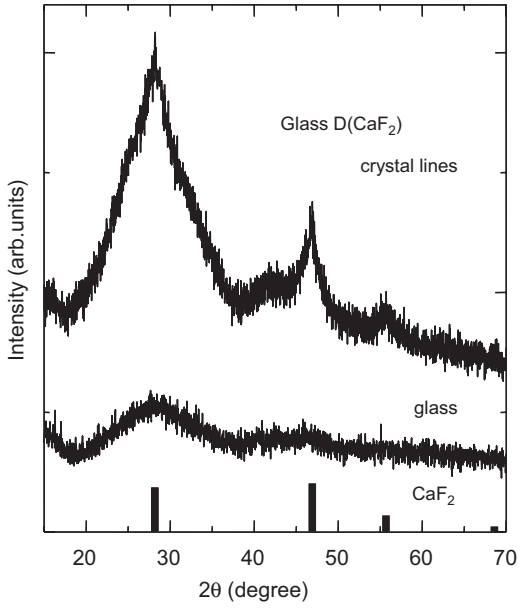

Fig. 9. XRD patterns at room temperature for the base glass and sample with 50 lines patterned by Yb:YVO_4 laser irradiations with a laser power of $P = 1.7$ W and a scanning speed of $S = 2\,\mu m/s$ in Glass D(CaF_2).

glasses of $43SiO_2$–$22Al_2O_3$–5CaO–13NaF–$17CaF_2$–3NiO–$0.5ErF_3$. This glass is designated here as Glass E(CaF_2). Laser irradiation experiments ($P = 1.7$ W and $S = 2\,\mu m/s$) were also carried out for Glass E(CaF_2), and lines with a morphology similar to Glass D(CaF_2) (Fig. 8) were patterned successfully. Micro-photoluminescence spectra at room temperature were measured for the line part (laser irradiated part) and the glassy part (not laser irradiated part), and the results are shown in Figs. 10 and 11. The excitation wavelength was 488 nm. Clear emissions

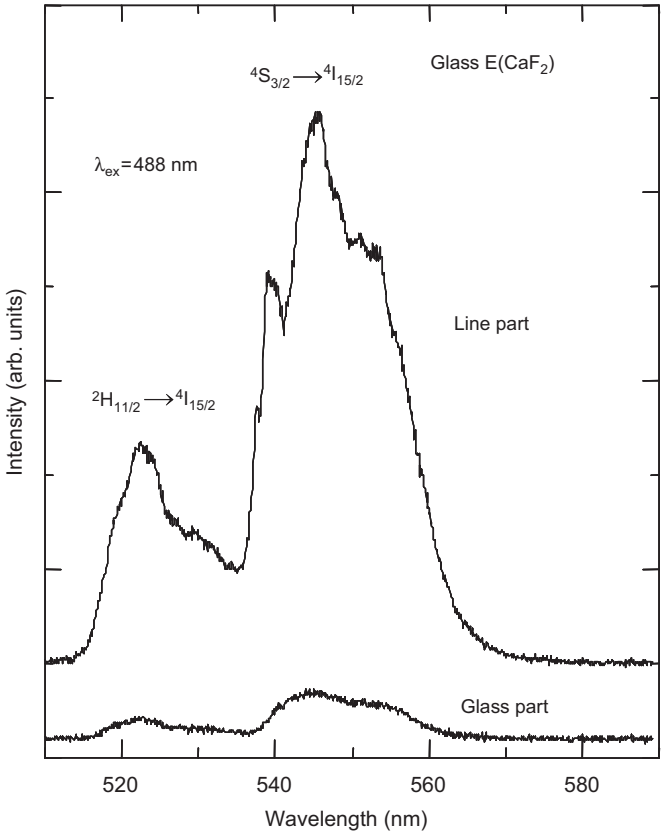

Fig. 10. Micro-photoluminescence spectra in the range of 510–590 nm at room temperature for the line part (laser irradiated part) patterned by Yb:YVO_4 laser irradiations with a laser power of $P = 1.7$ W and a scanning speed of $S = 2\,\mu m/s$ and the glassy part in Er^{3+}-doped Glass E(CaF_2). The wavelength of excitation lights is 488 nm.

corresponding to the *f*–*f* transition of $^2H_{11/2} \rightarrow {}^4I_{15/2}$, $^4S_{3/2} \rightarrow {}^4I_{15/2}$, and $^4F_{9/2} \rightarrow {}^4I_{15/2}$ in Er^{3+} ions are observed from the patterned lines. Furthermore, a Stark splitting was confirmed in these peaks. On the other hand, in the glass part, the intensity of emissions is extremely small or negligible. These results clearly demonstrate that Er^{3+} ions are incorporated into CaF_2 crystals being present in the lines patterned by laser irradiations. If Ni^{2+} ions are incorporated into CaF_2 nanocrystals, emission lights from Er^{3+} ions would be absorbed by Ni^{2+} ions (Fig. 1). The results shown in Figs. 10 and 11 suggest that the possibility of the incorporation of Ni^{2+} ions into Er^{3+}-doped CaF_2 crystals would be extremely small. Bensalah et al. [23] synthesized Er^{3+}-doped CaF_2 nanoparticles (~20 nm) using a reverse micelle method and measured the photoluminescence spectra (the excitation is 355 nm) of Er^{3+} ions. The spectra shown in Figs. 10 and 11 for the patterned lines with CaF_2 nanocrystals are similar to those reported by Bensalah et al. [23]. Furthermore, it is reported that the relative intensity of the green emission ($^2H_{11/2} \rightarrow {}^4I_{15/2}$ and $^4S_{3/2} \rightarrow {}^4I_{15/2}$) to the red emission ($^4F_{9/2} \rightarrow {}^4I_{15/2}$) increases with the decrease in the concentration of Er^{3+} ions incorporated into a given crystal [23–25]. As shown in Figs. 10 and 11, the green emission is

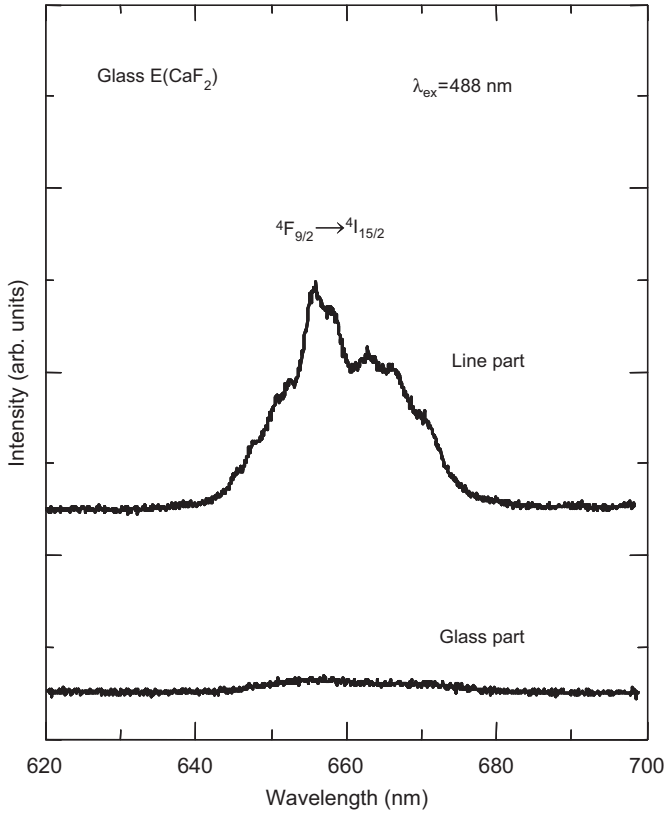

Fig. 11. Micro-photoluminescence spectra in the range of 620–700 nm at room temperature for the line part (laser irradiated part) patterned by Yb:YVO_4 laser irradiations with a laser power of $P = 1.7$ W and a scanning speed of $S = 2$ μm/s and the glassy part in Er^{3+}-doped Glass E(CaF_2). The wavelength of excitation lights is 488 nm.

dominant in the lines with CaF_2 nanocrystals patterned by laser irradiations, suggesting that the amount of Er^{3+} ions incorporated into CaF_2 nanocrystals would be small. In the present study, the precursor oxyfluoride glass, i.e, Glass E(CaF_2), contains the small concentration of $0.5ErF_3$, and this would be one of the reasons for the dominant green emission from the patterned line.

The present study demonstrates that it is possible to pattern spatially selected LaF_3 or CaF_2, and Er^{3+}-doped CaF_2 crystals on the surface of oxyfluoride glasses by laser irradiations. This demonstration would lead to further practical applications of oxyfluoride glasses such as fluoride-based optical waveguides. Of course, optical functional RE^{3+} ions must be incorporated into LaF_3 or CaF_2 nanocrystals in laser-induced crystal lines. Further studies on the patterning of laser-induced fluoride crystals with other RE^{3+} ions such as Nd^{3+}, Tm^{3+}, or Pr^{3+} and more detailed fluorescence properties are now under considerations.

3.5. Formation mechanism of LaF_3 and CaF_2 nanocrystals by laser irradiation

It is known that crystallization of glass proceeds through two steps of nucleation and crystal growth. The temperature dependence of nucleation and crystal growth rates in oxyfluoride glasses prepared in this study has not been clarified at this moment. It is, however, considered that the temperature dependence of nucleation and crystal growth rates for LaF_3 or CaF_2 nanocrystals is largely different from that for the host oxide glass part, because the strength of La^{3+}–F^- or Ca^{2+}–F^- bond is weak compared with cation–oxygen bonds such as Si^{4+}–O^2. This would be the reason why transparent oxyfluoride glasses with LaF_3 or CaF_2 nanocrystals have been fabricated easily through simple heat treatments of glasses in an electric furnace and the crystallization of the oxide glassy part occurs after the crystallization of fluoride nanocrystals. The model for the nucleation and crystal growth rates in oxyfluoride glasses is shown schematically in Fig. 12.

Even in the crystallization of oxyfluoride glasses by laser irradiations with conditions applied in this study, it is considered that only fluoride LaF_3 or CaF_2 crystals are formed. As indicated in Figs. 7–9, the glassy phase also exists in the laser-irradiated region besides LaF_3 or CaF_2 nanocrystals. Since SiO_2-based network structures in oxyfluoride glasses are considered to be extremely tight, oxide rich glassy phases based on SiO_2-based networks would remain in laser-irradiated regions without being excluded from the regions. This situation is the same as that in transparent oxyfluoride glasses consisting of fluoride nanocrystals prepared through the crystallization in an electric furnace. The lines patterned by laser irradiations in this study are, therefore, considered to be consisted of the composite of LaF_3 or CaF_2 nanocrystals and SiO_2-based oxide glassy phases as shown in Fig. 13 schematically.

In the technique applied in this study, irradiated lasers of Nd:YAG laser with $\lambda = 1064$ nm or Yb:YVO_4 fiber laser with $\lambda = 1080$ nm are absorbed by Ni^{2+} ions in the glasses through *d–d* transitions, and the absorbed energies are transferred to thermal energies through a non-radiative

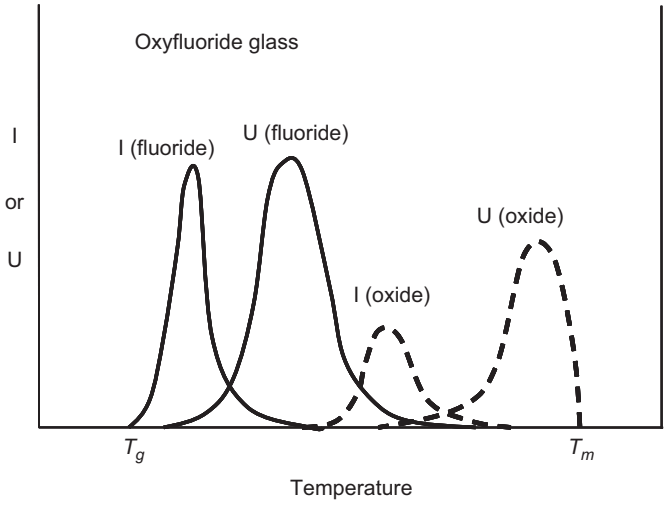

Fig. 12. Schematic model for the nucleation, *I*, and crystal growth, *U*, rates of fluoride nanocrystals and host oxide glass part in oxyfluoride glasses. T_g and T_m are the glass transition and melting temperatures, respectively.

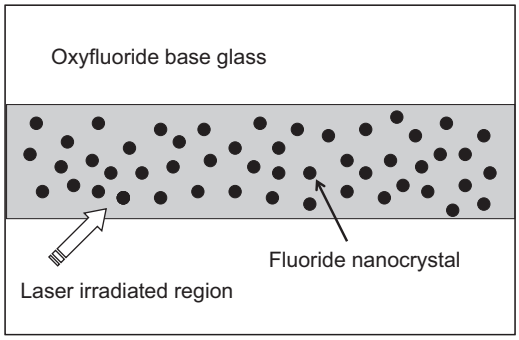

Fig. 13. Schematic model for the laser irradiated region in oxyfluoride glass. The line consists of the composite of fluoride nanocrystals and host oxide glassy phase.

relaxation process (electron–phonon couplings). And thus the surroundings of Ni^{2+} ions are heated, consequently inducing effective crystallizations in the glasses. This technique has, therefore, a high potential for spatially selected crystallizations in various types of glasses even in oxyfluoride glasses as demonstrated in this study. In this sense, it is also of interest to pattern fluoride crystals by laser irradiations in oxyfluoride glasses containing a small amount of oxides. In such glasses, patterning of lines consisting of highly oriented fluoride crystals (not nanocrystals) might be possible.

4. Conclusions

The oxyfluoride glasses such as $40SiO_2$–$25Al_2O_3$–$20Na_2O$–$15LaF_3$–3NiO with a small amount of NiO were prepared, and irradiations of cw lasers with $\lambda = 1064$ or 1080 nm were performed to induce the spatially selected crystallization of LaF_3 and CaF_2 crystals on the glass surface. The dots and lines consisting of LaF_3 or CaF_2 crystals were patterned successfully. The line patterning with Er^{3+}-doped CaF_2 crystals was also confirmed from micro-photoluminescence spectrum measurements, in which clear fluorescence emissions typical of Er^{3+} ions embedded in fluoride crystals were observed. It was proposed that the lines patterned by laser irradiations in this study are the composite of LaF_3 or CaF_2 nanocrystals and SiO_2-based oxide glassy phase. It was demonstrated that a combination of Ni^{2+}-dopings and laser irradiations is effective in spatially selected local crystallizations of fluorides in oxyfluoride glasses.

Acknowledgments

This work was supported from the Grant-in-Aid for Scientific Research from the Ministry of Education, Science, Sports, Culture, and Technology, Japan.

References

[1] Y. Wang, J. Ohwaki, Appl. Phys. Lett. 63 (1993) 3268.
[2] M.J. Dejneka, J. Non-Cryst. Solids 239 (1998) 149.
[3] S. Tanabe, H. Hayashi, T. Hanada, N. Onodera, Opt. Mater. 19 (2002) 343.
[4] R.S. Meltzer, H. Zheng, M.J. Dejneka, J. Lumin. 107 (2004) 166.
[5] H. Zheng, X.J. Wang, M.J. Dejneka, W.M. Yen, R.S. Meltzer, J. Lumin. 108 (2004) 395.
[6] X. Qiao, X. Fan, J. Wang, M. Wang, J. Non-Cryst. Solids 351 (2005) 357.
[7] E. Ma, Z. Hu, Y. Wang, F. Bao, J. Lumin. 118 (2006) 131.
[8] D. Chen, Y. Wang, Y. Yu, E. Ma, F. Liu, J. Phys. Chem. Solids 68 (2007) 193.
[9] M. Mortier, A. Bensalah, G. Dantelle, G. Patriarche, D. Vivien, Opt. Mater. 29 (2007) 1263.
[10] T. Honma, Y. Benino, T. Fujiwara, T. Komatsu, R. Sato, Appl. Phys. Lett. 83 (2003) 2796.
[11] T. Honma, Y. Benino, T. Fujiwara, T. Komatsu, R. Sato, Appl. Phys. Lett. 88 (2006) 231105.
[12] M. Abe, Y. Benino, T. Fujiwara, T. Komatsu, R. Sato, J. Appl. Phys. 97 (2005) 123516.
[13] R. Ihara, T. Honma, Y. Benino, T. Fujiwara, R. Sato, T. Komatsu, Solid State Commun. 136 (2005) 273.
[14] T. Komatsu, R. Ihara, T. Honma, Y. Benino, R. Sato, H.G. Kim, T. Fujiwara, J. Am. Ceram. Soc. 90 (2007) 699.
[15] H. Sugita, T. Honma, Y. Benino, T. Komatsu, Solid State Commun. 143 (2007) 280.
[16] M. Sato, T. Honma, Y. Benino, T. Komatsu, J. Solid State Chem. 180 (2007) 2541.
[17] S.E. Mekhlouf, A. Boukenter, M. Ferrari, F. Goutaland, N. Ollier, Y. Ouerdane, J. Non-Cryst. Solids 353 (2007) 506.
[18] J.S. Berks, W.B. White, Phys. Chem. Glasses 7 (1966) 191.
[19] D. Möncke, D. Ehrt, Glastech. Ber. Glass Sci. Technol. 74 (2001) 199.
[20] F.H.A. Elbatal, M.M.I. Khalil, N. Nada, S.A. Desouky, Mater. Chem. Phys. 82 (2003) 375.
[21] G. Lakshminarayana, S. Buddhudu, Spectrochim. Acta A 63 (2006) 295.
[22] R.D. Shannon, Acta Cryst. A 32 (1976) 751.
[23] A. Bensalah, M. Mortier, G. Patriarche, P. Gredin, D. Vivien, J. Solid State Chem. 179 (2006) 2636.
[24] P.S. Golding, S.D. Jackson, T.A. King, M. Pollnau, Phys. Rev. B 62 (2000) 856.
[25] A. Patra, C.S. Friend, R. Kapoor, P.N. Prasad, Chem. Mater. 15 (2003) 3650.